PAPER

Influence of material stretchability on the equilibrium shape of a Möbius band†

David M. Kleiman,[a] Denis F. Hinz,[b] Yoichi Takato[c] and Eliot Fried*[c]

We use a two-dimensional discrete, lattice-based model to show that Möbius bands made with stretchable materials are less likely to crease or tear. This stems from a delocalization of twisting strain that occurs if stretching is allowed. The associated low-energy configurations provide strategic target shapes for the guided assembly of nanometer and micron scale Möbius bands. To predict macroscopic band shapes for a given material, we establish a connection between stretchability and relevant continuum moduli, leading to insight regarding the practical feasibility of synthesizing Möbius bands from materials with continuum parameters that can be measured experimentally or estimated by upscale averaging.

1 Introduction

Recent technical advances have made it increasingly clear that the properties of a material are determined not only by its composition but also by geometrical and topological factors.[1] With this realization and breakthroughs in the ability to fabricate objects with molecular-scale precision, research into using the one-sided topology of the Möbius band in scientific applications is burgeoning. In chemical topology, for example, mechanically interlinked molecules, or catenanes, have been created using Möbius molecules as intermediaries, setting the stage for the synthesis of programmable topological nanostructures.[2,3] Micron-scale Möbius crystals, which were first created over a decade ago by spooling niobium triselenide ribbons onto selenium droplets,[4] can be viewed as global disclinations.[5] The ability of a recently synthesized expanded porphyrinoid to switch between Hückel and Möbius topologies presents the possibility of novel memory devices.[6,7] Möbius topology is also

exhibited by cyclotides, macrocyclic plant proteins involved in plant defense.[8] Due to their topologically derived structural stability, these proteins have the potential to serve as drug scaffolds and pharmaceutical templates.[9–11]

This article focuses on the problem of computing energetically preferred equilibrium shapes of Möbius bands. This direction was initiated by Sadowsky,[12–17] who considered materials like paper which are easy to bend but essentially unstretchable and, thus, must adopt shapes that are very closely approximated by developable surfaces. Aside from proving that it is possible to construct a developable band from a rectangular strip of width sufficiently small relative to its length, Sadowsky established an upper bound for the bending energy of a developable band and derived a dimensionally reduced expression for the bending energy of a band made from an infinitesimally thin rectangular strip. Wunderlich[18,19] later sharpened Sadowsky's bound and generalized Sadowsky's bending energy to incorporate the effect of finite width. The problem of constructing developable equilibrium configurations was first considered by Mahadevan and Keller,[20] whose numerically determined solutions led to a tighter upper bound on the bending energy but are inconsistent with results of Randrup and Røgen,[21] who showed that the midline of a Möbius band must have an odd number of switching points at which its curvature and torsion both vanish. Using Wunderlich's energy, Starostin and van der Heijden[22,23] computed equilibria that meet these requirements and also found evidence to suggest that Sadowsky's energy is a singular limit that produces midlines with discontinuous curvatures.

We depart from established tradition and explore the influence of material stretchability on the shape of an equilibrated Möbius band. For bands with sufficiently large width-to-length ratios, Starostin and van der Heijden[22,23] observed localized zones of concentrated bending-energy density. Their results point to the emergence of singularities indicative of the onset of failure.

[a] *Department of Mathematics and Statistics, McGill University, Montréal, Québec, Canada H3A 2K6. E-mail: dave.kleiman2@gmail.com; Tel: +1 514 516 0778*

[b] *Kamstrup A/S, Industrivej 28, Stilling, 8660 Skanderborg, Denmark. E-mail: dfhinz@gmail.com; Fax: +45 89 93 10 01; Tel: +45 2480 4870*

[c] *Mathematical Soft Matter Unit, Okinawa Institute of Science and Technology Graduate University, Onna, Okinawa, Japan 904-0495. E-mail: yoichi.takato@oist.jp, eliot.fried@oist.jp; Fax: +81 (0)98 966 1062; Tel: +81 (0)98 966 1318*

† Electronic supplementary information (ESI) available: The supporting movie aspectRatio_4pi.mp4 shows three-dimensional views of bands with $a = 4\pi$ and different γ as shown in Fig. 2; the supporting movie aspectRatio_pi.mp4 shows three-dimensional views of bands with $a = \pi$ and different γ as shown in Fig. 2; the supporting movie gamma_7.mp4 shows three-dimensional views of bands with $\gamma = 3.0\pi \times 10^{7/12}$ and different a as shown in Fig. 2; the supporting movie gamma_42.mp4 shows three-dimensional views of bands with $\gamma = 3.0\pi \times 10^{21/6}$ and different a as shown in Fig. 2; the supporting movie gamma_84.mp4 shows three-dimensional views of bands with $\gamma = 3.0\pi \times 10^7$ and different a as shown in Fig. 2. See DOI: 10.1039/c5sm02188j

Even a slight degree of stretchability should alleviate such concentrations. We seek to quantify both this effect and accompanying shape variations that bands of different aspect ratios exhibit with increasing stretchability. In this connection, a model that allows for small but discernible stretchability applies even to conventional paper, which stretches by a percent or two in the direction of loading without creasing or tearing.[24]

Our approach utilizes a discrete, lattice-based model that incorporates stretching but can also accurately approximate developable shapes for sufficiently small values of the stretchability. Regardless of the aspect ratio of the band, we find that the total energy decreases monotonically with stretchability. This strongly suggests that bands made of stretchable materials might be easier to form than bands made of unstretchable materials.

For further insight regarding how stretchability influences equilibrium shape, we compute the mean and Gaussian curvatures for bands of various length-to-width aspect ratios, the latter of which is nonzero only for stretchable materials.[25] Consistent with the observation that unstretchable materials must adopt developable shapes, we find that the Gaussian curvature plays a key role in bands comprised of such materials. Except for cases involving combinations of the smallest aspect ratio and the two largest values of stretchability investigated, the mean and Gaussian curvatures distribute more evenly with increased stretchability. Bending is concomitantly transferred to stretching, thereby eliminating localized zones of concentrated bending-energy density.

We also show that our model is energetically consistent with a simple continuum theory and derive links between our material parameters and those of the continuum theory. These links could provide a basis for future material design and applications.

2 Discrete, lattice-based model

We first provide a brief description of our model. Additional details are provided in the ESI.†

2.1 Kinematics

The shape of a Möbius band made from an unstretchable material is uniquely determined (up to a rigid transformation) by the curvature κ and torsion τ of its midline.[12,13] This shape must be developable. That is, it must be a ruled surface that can be continuously flattened onto a planar region without stretching or contracting. In contrast, a band made of a stretchable material can adopt a nondevelopable equilibrium shape uniquely determined (up to a rigid transformation) by the corresponding first and second fundamental forms, as discussed in the ESI.†

2.2 Linear and angular springs

We approximate a rectangular strip of length L and width w by a lattice of equilateral triangles with N points uniformly separated by a distance r_0. To incorporate resistance to stretching, we connect each pair of lattice points by a linear spring with stiffness k_l and equilibrium length $r_e = r_0$. Further, to incorporate resistance to out-of-plane bending, we connect each triplet of lattice points with a torsional spring of stiffness $k_\theta > 0$ and equilibrium angle $\theta_e = \pi$. The total energy E of the band is then given by the sum

$$E = \frac{k_l}{2} \sum_{i \in S_l} (r(i) - r_e)^2 + \frac{k_\theta}{2} \sum_{i \in S_\theta} (\theta(i) - \theta_e)^2, \quad (1)$$

where S_l and S_θ denote the sets of all linear and torsional springs, $r(i)$ is the length of the i-th linear spring, and $\theta(i)$ is the angle between triplets of points associated with the i-th torsional spring.

2.3 Nondimensionalization

The width w, length L, linear spring constant k_l, and angular spring constant k_θ yield dimensionless parameters

$$a = \frac{L}{w} \quad \text{and} \quad \gamma = \frac{k_l L w}{k_\theta}. \quad (2)$$

While a is simply the (length-to-width) aspect ratio of the strip, the Föppl–von Kármán (FvK) number γ measures the resistance of the strip to stretching relative to its resistance to bending.[26] Small values of γ describe stretchable materials. Larger values of γ describe materials like paper, graphene, and DNA which bend easily but are difficult to stretch. The case $\gamma \to \infty$ of infinite FvK number corresponds to the idealized limit of a material which cannot be stretched and thus can adopt only developable shapes.

To nondimensionalize the total energy of the band, we first note that, for a large number of points N on the band, $Lw \approx 4N r_e^2 / \sqrt{3}$, where r_e is the equilibrium length of a linear spring, as N asymptotically approaches the number of lattice unit cells. We also note that, upon increasing N for a fixed shape, the energy decreases inversely proportionately to N, since the angular deflection of each torsional spring and deformation of each linear spring relative to the length of the band decreases inversely proportionately to N. Next, using k_θ/a as a reference energy (the effective angular spring constant, since the number of springs in series is proportional to a), normalizing by N, and defining

$$\Psi = \frac{EaN}{k_\theta}, \quad \text{and} \quad \tilde{r}(i) = \frac{r(i)}{r_e}, \quad (3)$$

leads to a dimensionless version

$$\Psi = \Psi_s + \Psi_b \quad (4)$$

of the total energy (1), with stretching and bending contributions

$$\Psi_s = 2a\gamma \sum_{i \in S_l} \frac{(\tilde{r}(i) - 1)^2}{\sqrt{3}} \quad \text{and} \quad \Psi_b = Na \sum_{i \in S_\theta} \frac{(\theta(i) - \theta_e)^2}{2}. \quad (5)$$

For brevity, the dimensionless quantities Ψ, Ψ_s, and Ψ_b are hereafter referred to as energies.

A conjugate-gradient method within the molecular dynamics code LAMMPS[27] (Large-scale Atomic/Molecular Massively Parallel Simulator) is used to minimize Ψ. For all values of the aspect ratio a considered, trial shapes are provided by Sadowsky's piecewise isometric construction (Fig. 1).[12,13] Since each such shape is developable, minimizing the energy of a band made of a material
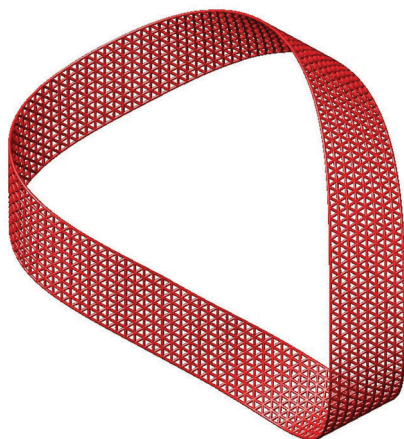
Fig. 1 Schematic of a trial configuration provided by Sadowsky's[12,13] developable Möbius band and used for computing the energetically preferred shape of a band of aspect ratio $a = 6\pi$ discretized by $N = 1170$ points separated by uniform dimensionless distance $r_0/L = \sqrt{3}/72\pi$.

with sufficiently large FvK number γ constrains stretching and thus maintains approximate developability. With the linear springs at their equilibrium distance, this minimization amounts to reducing the curvature of the band without altering the distances between points on the lattice. Conversely, the spacing between lattice points is unconstrained for sufficiently small values of γ. The model and energy minimization strategy have been subjected to extensive validation procedures, as described in the ESI.†

3 Simulation results

Our simulations indicate that stretchable Möbius bands adopt two characteristic equilibrium shapes, depending on the combination of FvK number γ and aspect ratio a. For sufficiently large values of γ, the bands take shapes essentially indistinguishable from those of paper models and previous simulation results. Deviations from developability increase as γ decreases.

3.1 Equilibrium shapes

Equilibrium band shapes obtained by minimizing the total energy Ψ for representative combinations of γ and a appear in Fig. 2.

For sufficiently large values of γ and each value of a considered, equilibrium shapes qualitatively resemble those of model bands made from rectangular strips of paper and thus appear to be nearly developable. Regardless of the value of a, increasing γ appears to have a negligible influence above $\gamma = 3.0\pi \times 10^{14/3}$. However, the influence of γ becomes progressively more evident below $\gamma = 3.0\pi \times 10^{14/3}$ and is increasingly obvious for smaller values of a. The midlines of bands appear to be more circular and less out of plane for smaller values of γ, an impression that is confirmed by plots for bands of aspect ratio $a = 2\pi$ that appear in Fig. 3.

If γ is sufficiently large, the tangent vector to the midline of each equilibrated band exhibits an odd number of switching points at which its curvature κ and torsion τ vanish simultaneously.

While κ has two peaks and one zero, τ has two peaks and three zeroes (Fig. 4). These observations are consistent with previous analytical and numerical results.[21–23] Moreover, for smaller values of a, the peak values of κ and τ are larger. In keeping with findings of Mahadevan and Keller[20] and Starostin and van der Heijden,[22,23] the midlines of these bands are more out-of-plane than those of bands with larger aspect ratios (Fig. 5). Comprehensive convergence and validation studies in the unstretchable limit $\gamma \to \infty$ are provided in the ESI.†

3.2 Degenerate equilibrium shapes and model limitations

For $a = \pi$, bands made of materials with FvK number $\gamma = 3.0\pi$ (Fig. 2) and $\gamma = 3.0\pi \times 10^{7/12}$ (Fig. 8) exhibit degenerate equilibrium shapes that represent a breakdown of the Möbius topology.

The band with FvK number $\gamma = 3\pi \times 10^{7/12}$ exhibits a self-intersecting achiral shape resembling the collapse observed in Möbius soap films with small throat distances.[28] However, the constraint of lattice connectivity inherent to our model delivers shapes different from those of collapsed Möbius soap films.

Further decreasing the FvK number to $\gamma = 3.0\pi$ results in a flat, annular shape with curvature and stretching energy concentrated along its edges (Fig. 8). This configuration is achieved through collapsing (or folding) the self-intersecting achiral shape to lie in a plane. The result is a double-layered two-dimensional annulus with a width approximately half of the band width of the trial configuration.

These degenerate shapes, which are possible only if interpenetration of the lattice is allowed, suggest that for sufficiently small values of the aspect ratio a the Möbius topology is unattainable unless the FvK is sufficiently large.

3.3 Energy measures

Plots of the stretching energy Ψ_s, the bending energy Ψ_b, and the total energy Ψ are provided in Fig. 6 for representative combinations of γ and a.

For each choice of a, the stretching energy Ψ_s exhibits small but finite values for large FvK numbers and vanishes in the unstretchable limit $\gamma \to \infty$. In contrast, for a range of intermediate FvK numbers, Ψ_s varies significantly for different values of a. For sufficiently small values of a, Ψ_s exhibits one maximum at intermediate FvK numbers. However, for sufficiently large values of a, Ψ_s exhibits two local maxima.

The total energy Ψ is dominated by the order-of-magnitude larger Ψ_b, which decreases monotonically for decreasing γ. Hence, the sum $\Psi = \Psi_s + \Psi_b$ decreases monotonically as γ decreases and the minimum value of Ψ for any band is attained at the smallest value of γ considered.

From an energetic perspective, it therefore seems reasonable to infer that bands made of stretchable materials are significantly less costly to make than bands made of unstretchable materials.

The influence of a on Ψ becomes most evident for large values of γ. For large values of γ, Ψ decreases monotonically as a increases. Most notably, below a critical value $\gamma_c \sim 10^3$ of γ,
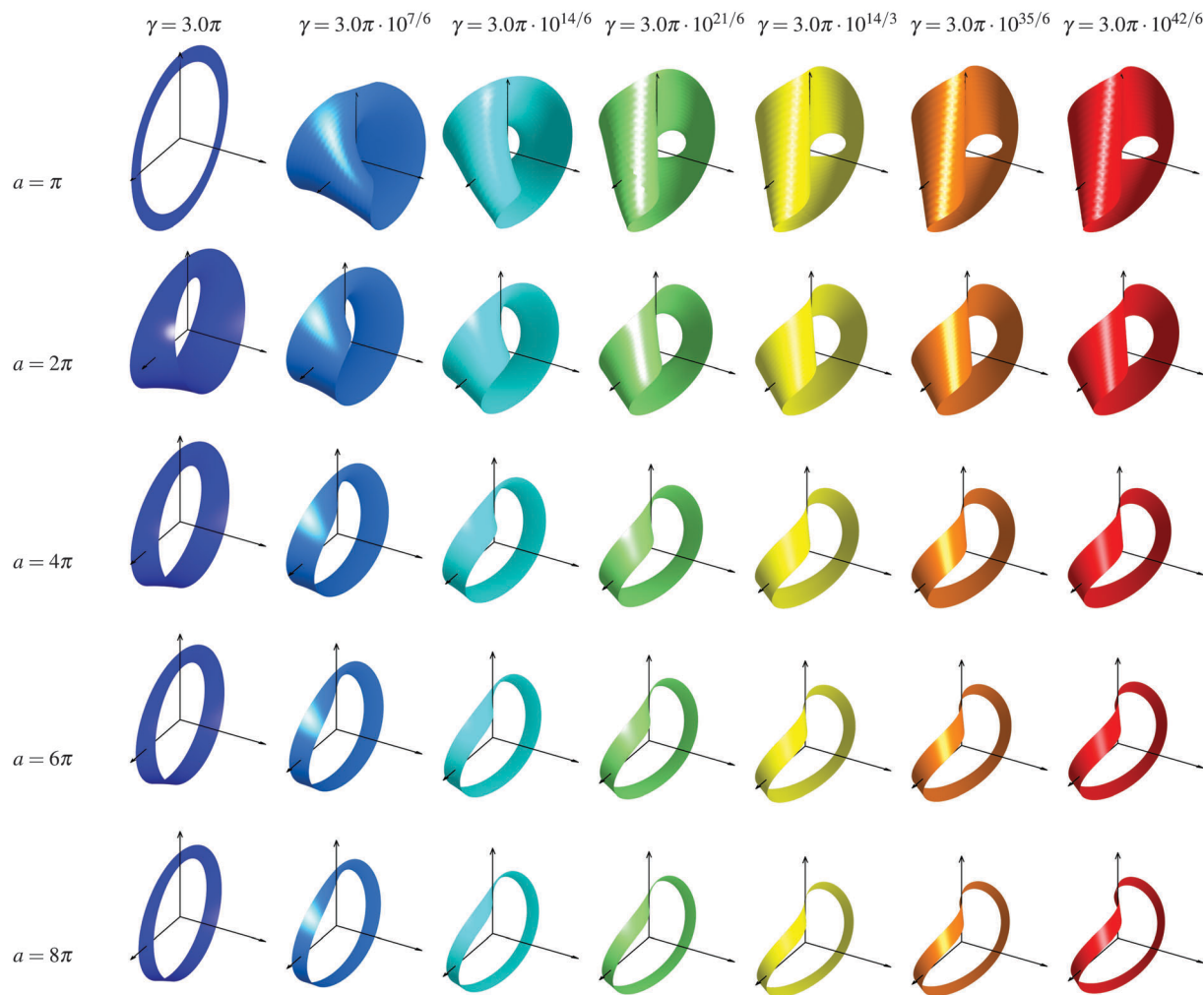
Fig. 2 Möbius bands adopt characteristic equilibrium shapes depending on FvK number γ and aspect ratio a: equilibrium shapes for various values of γ and a. Bands are rotated into their main axes. For other perspective views, see ESI,† Fig. S7.
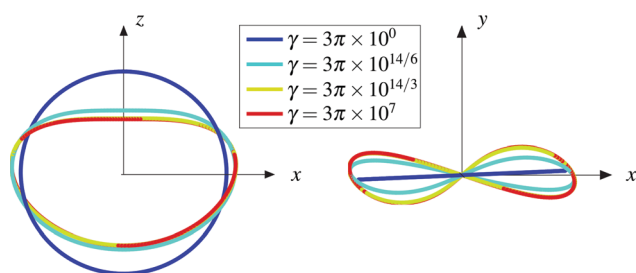

Fig. 3 Centerlines of equilibrated bands with aspect ratio $a = 2\pi$ made from materials of various values of the FvK number γ.

Fig. 4 In the unstretchable limit $\gamma \to \infty$, the model recovers analytical predictions of Randrup and Røgen[21] and the characteristic shape obtained by Starostin and van der Heijden.[22,23] Curvature κ and torsion τ of the midline of Möbius bands for FvK number $\gamma = 3\pi \times 10^7$ and various values of the aspect ratio a versus the arclength along the midline in terms of the number N_l of points along the midline.

the total energies of bands with different a coincide, indicating that Ψ becomes essentially independent of the aspect ratio.

This effect is in agreement with everyday experience: the effort needed to twist a rectangular sheet of an essentially unstretchable material like paper into a Möbius band increases notably as its length-to-width aspect ratio deceases. Moreover, performing the same task with a stretchable material, such as a
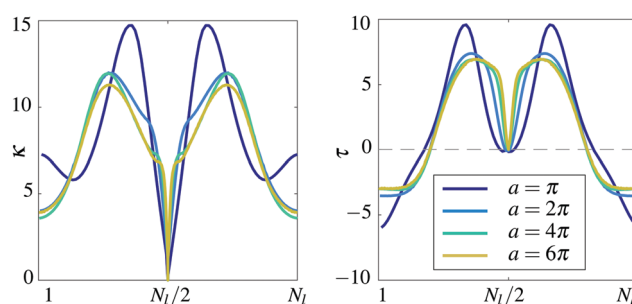
thin sheet of rubber, is much easier. More quantitatively, our results reveal that the energy of bands with small a increases approximately linearly with $\log \gamma$ over a wide region from
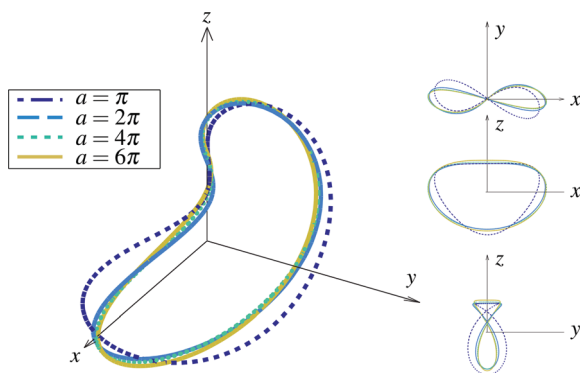
Fig. 5 The shape of the midline of an effectively unstretchable Möbius band depends on its aspect ratio a: Centerlines of equilibrium shapes of Möbius bands for FvK number $\gamma = 3\pi \times 10^7$ and representative values of a. Bands are rotated into their main axes as in Fig. 2.
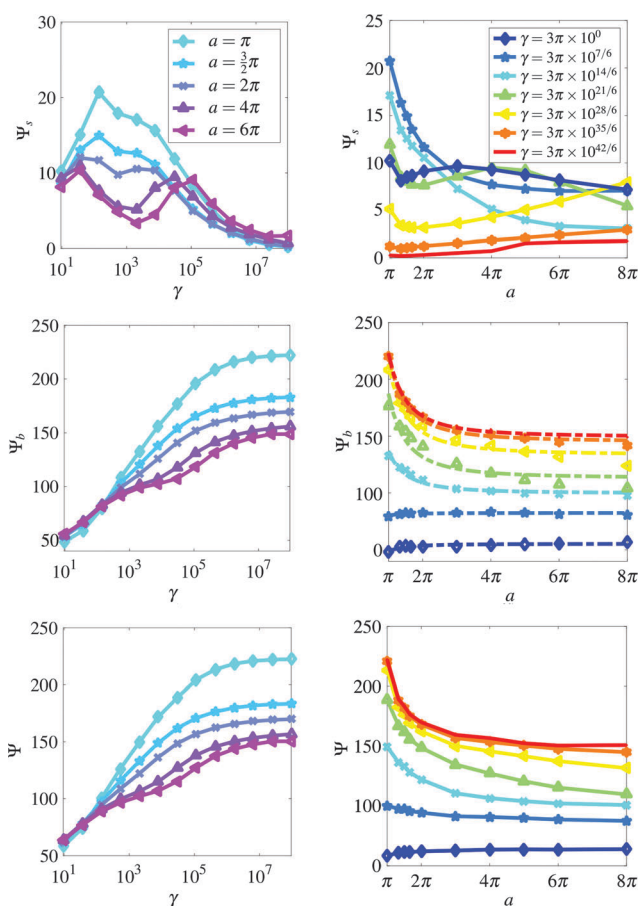

Fig. 6 Stretching energy Ψ_s, bending energy Ψ_b, and total energy Ψ for representative combinations of FvK number, γ, and aspect ratio, a.

$\gamma \approx 10.0$ to $\gamma \approx 10^5$. Bands with larger a also exhibit a smaller region of approximate linearity with $\log \gamma$ from $\gamma \approx 10.0$ to $\gamma \approx 10^3$, but the energy saturates for larger γ.

The collapsed shapes of the present model with unpenalized self-intersections are observed for combinations of small γ and small a where the stretching energy attains values of magnitude comparable to that of the bending energy.

With reference to the previously noted observation that the midlines of bands become more circular and less out-of-plane with decreasing γ, the observed dependence of Ψ on γ indicates that more planar, less bent configurations are energetically favored below a certain critical FvK number. For the particular choice $\gamma = 3.0\pi \times 10^7$, Ψ_s is negligibly small compared to Ψ_b and, thus, $\Psi \sim \Psi_b$. The choice $\gamma = 3.0\pi \times 10^7$ therefore suffices to capture the strictly unstretchable limit $\gamma \to \infty$. The synthesis of Möbius bands is challenging mainly due to their significantly higher energy states relative to untwisted rings. However, allowing for stretching reduces this difference and could therefore diminish the difficulty of fabrication strategies that rely on bending rectangular strips.

Since Ψ decreases as γ decreases for each value of a considered, the loss of chirality exhibited by bands of aspect ratio $a = \pi$ made from materials with FvK number $\gamma = 3.0\pi$ and $\gamma = 3.0\pi \times 10^{7/12}$ indicates that chiral shapes have larger stored energies. To fabricate chiral objects, a system must therefore be sufficiently and properly constrained. For example, anisotropic particles can be used to guide the assembly of chiral objects.[29] Our results indicate that small aspect ratio Möbius bands made from a material that is too stretchable are likely to be unstable. On this basis, they suggest the existence of a threshold for FvK number above which the synthesis or guided assembly of small aspect ratio Möbius bands should become feasible.

3.4 Curvature and dilatation

In the ESI,† we show that the coarse-grained limit of our model corresponds to a continuum model for a surface S that resists stretching and bending. Whereas stretching is characterized by an area modulus μ_a related to the linear spring stiffness k_1 by

$$\mu_a = \frac{\sqrt{3}k_1}{2}, \qquad (6)$$

bending is characterized by splay and saddle-splay moduli μ and $\bar{\mu}$ related to the torsional spring stiffness k_θ by

$$\mu = \frac{3\sqrt{3}k_\theta}{2} \quad \text{and} \quad \bar{\mu} = -\frac{2\mu}{3} = -\sqrt{3}k_\theta. \qquad (7)$$

With (6) and (7), the total energy $\mathscr{E}$ of S takes the form

$$\mathscr{E} = \sqrt{3} \int_S \left[k_1 \varepsilon^2 + k_\theta (3H^2 - K) \right] \mathrm{d}a, \qquad (8)$$

where $\mathrm{d}a$ denotes the area element on S and where ε^2, H, and K denote the (two-dimensional) dilatation, mean curvature, and Gaussian curvature of S. The expression (6) for the area modulus μ_a is consistent with a result obtained by Seung and Nelson.[30] The bending contribution to (8) arising from (7), which is identical to that of a Kirchhoff plate with bending modulus $3\sqrt{3}k_\theta/2$ and Poisson's ratio 1/3, coincides with an expression derived by Merchant and Keller.[31]

The connection (6)–(8) suggests that the pointwise distributions of discrete approximations to H^2, K, and ε^2 may provide further insight regarding how the FvK number γ and aspect ratio a influence the shape of a Möbius band. Plots of these distributions are provided in Fig. 7 for representative values

of γ and a. To compute discrete versions of H^2 and K, we proceed by analogy to the continuous case,[32] where tangent vectors are approximated by vectors between neighboring points on the surface. In the effectively unstretchable limit $\gamma = 3.0\pi \times 10^7$, each band exhibits a nearly flat triangular region bounded at its vertices by zones in which H^2 takes large values and is surrounded by a nearly flat trapezoidal region. This is compatible with previous results,[14–17] as is the increase in size of the zones in which H^2 exhibits large values with increasing a. However, as γ decreases, H^2 becomes increasingly more evenly distributed over the band. Consistent with the observation that localized regions of concentrated bending-energy density indicate where creasing or tearing may occur,[22,23] our findings

show that for bands of small aspect ratio increasing the stretchability alleviates such concentrations.

All equilibrated bands exhibit non-vanishing Gaussian curvature K. However, for $\gamma = 3.0\pi \times 10^7$, K is very close to zero almost everywhere. This confirms that the choice $\gamma = 3.0\pi \times 10^7$ yields nearly developable shapes and thus provides a good approximation of the unstretchable limit, even though some degree of stretching is allowed for any value of $\gamma > 0$. For all of the smaller values of γ considered, H^2 and $|K|$ are maximized at the same points. The maximum values of $|K|$ become more prominent as a decreases. At the vertices of the previously discussed flat, triangular regions, where the contribution to the bending energy from H^2 is largest, the contribution to the
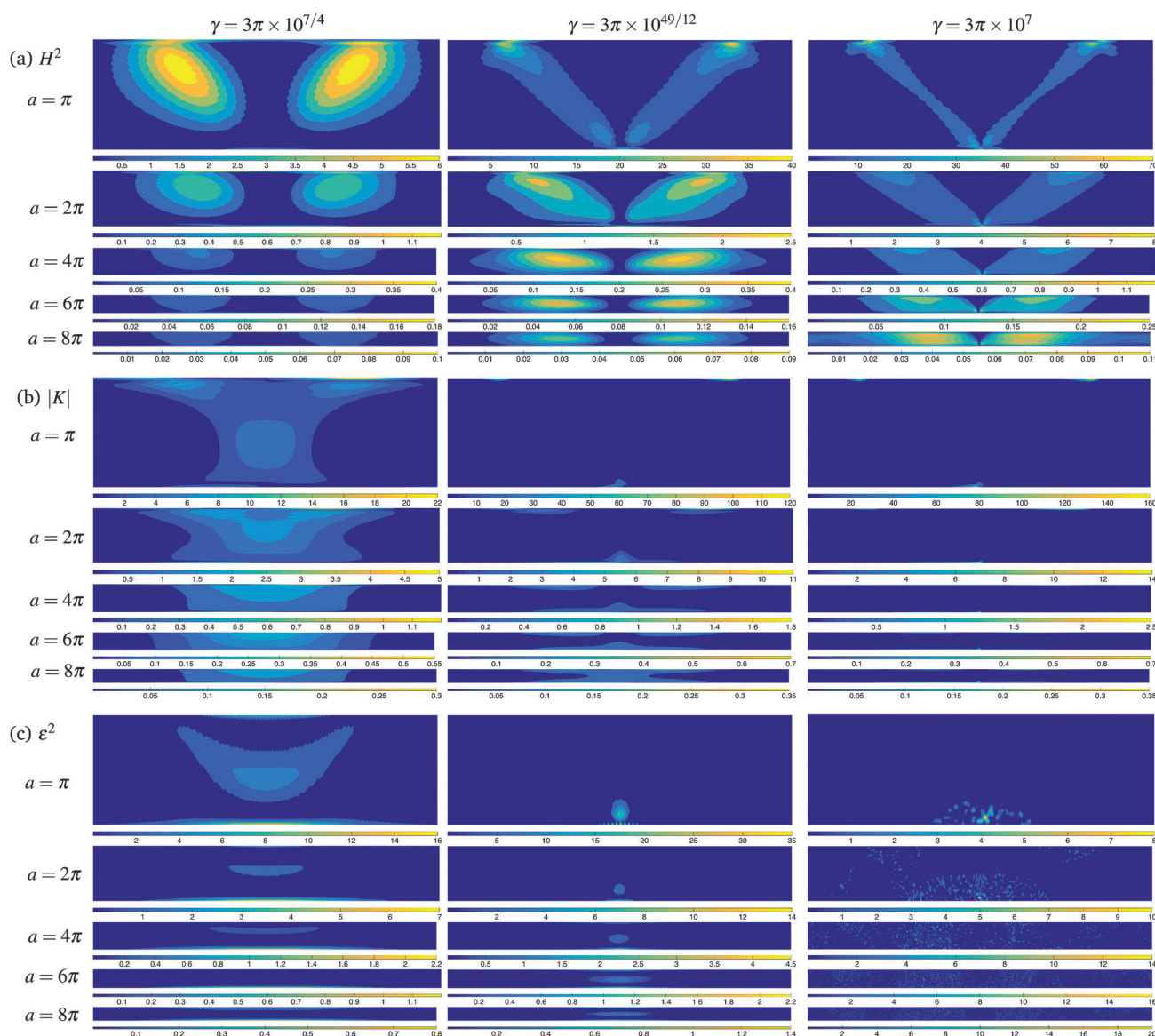
Fig. 7 The mean and Gaussian curvatures are both more evenly distributed for increasing stretchability (decreasing FvK number γ): (a) square H^2 of the mean curvature H, (b) magnitude $|K|$ of the Gaussian curvature K, and (c) square ε^2 of the strain ε of Möbius bands made of stretchable materials for various values of the aspect ratio a and γ. The aspect ratio of each contour plot equals that of the band it represents. Images of the bands corresponding to the contour plots appear in Fig. 2. Different scales are adapted individually to capture the entire range of relevant values. Additional cases appear in ESI,† Fig. S8.
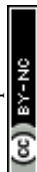
bending energy from $|K|$ also attains its largest values. Thus, even in the approximately unstretchable limit, it is favorable to locally transfer energy associated with H^2 to energy associated with K. Inspecting the local dilatation ε^2 shows that bending is locally transferred to stretching unless $K \equiv 0$, in which case the band adopts a genuinely developable shape. Since most materials manifest some in-plane elasticity, our findings also indicate that an actual band should possess a region of local stretching. This also suggests that loci of large H^2 are likely to lie within zones where the bending contribution to the energy is concentrated. These zones are also most likely to be sites for inelastic deformation or failure. Conversely, allowing for local stretching can reduce the bending contribution to the energy density.

Both H^2 and $|K|$ become more evenly distributed over the band with decreasing γ, resulting in lower curvature gradients. Further, both $|K|$ and ε^2 are transferred from the edge toward the midline of the band, reducing the magnitude of the gradient of the continuum bending-energy density and decreasing the likelihood of creasing or tearing accordingly. Nonzero values

of $|K|$ indicate that stretching contributes significantly to the overall shape of the band, as zones in which $|K|$ is largest coincide with zones of large ε^2, to which the continuum stretching-energy density (see the ESI†) is directly related. This result confirms the previous observation that decreasing γ yields bands with midlines that are more circular and less out-of-plane, and, thus, leads to a reduction of the bending energy. A zone of low bending energy is maintained as γ decreases. The magnitude $|K|$ of K is largest in zones where H^2 takes large values, resulting in large values of the continuum bending-energy density. However, this effect is mitigated by reduced gradients allowed by stretching.

The transition from bending to stretching occurs smoothly except for combinations of γ and a that lead to degenerate collapsed, achiral equilibrium shapes. Fig. 8 provides plots of H^2, $|K|$, and ε^2 for $a = \pi$ and the two smallest values of γ considered. For $\gamma = 3.0\pi \times 10^{7/12}$, H^2 and $|K|$ appear to diverge at a single point along the intersection and decay quickly with increasing distance from that point. The value of ε^2 is also greatest at the point in question but does not decay as rapidly. For $\gamma = 3.0\pi$, which results in a further collapse, by folding,
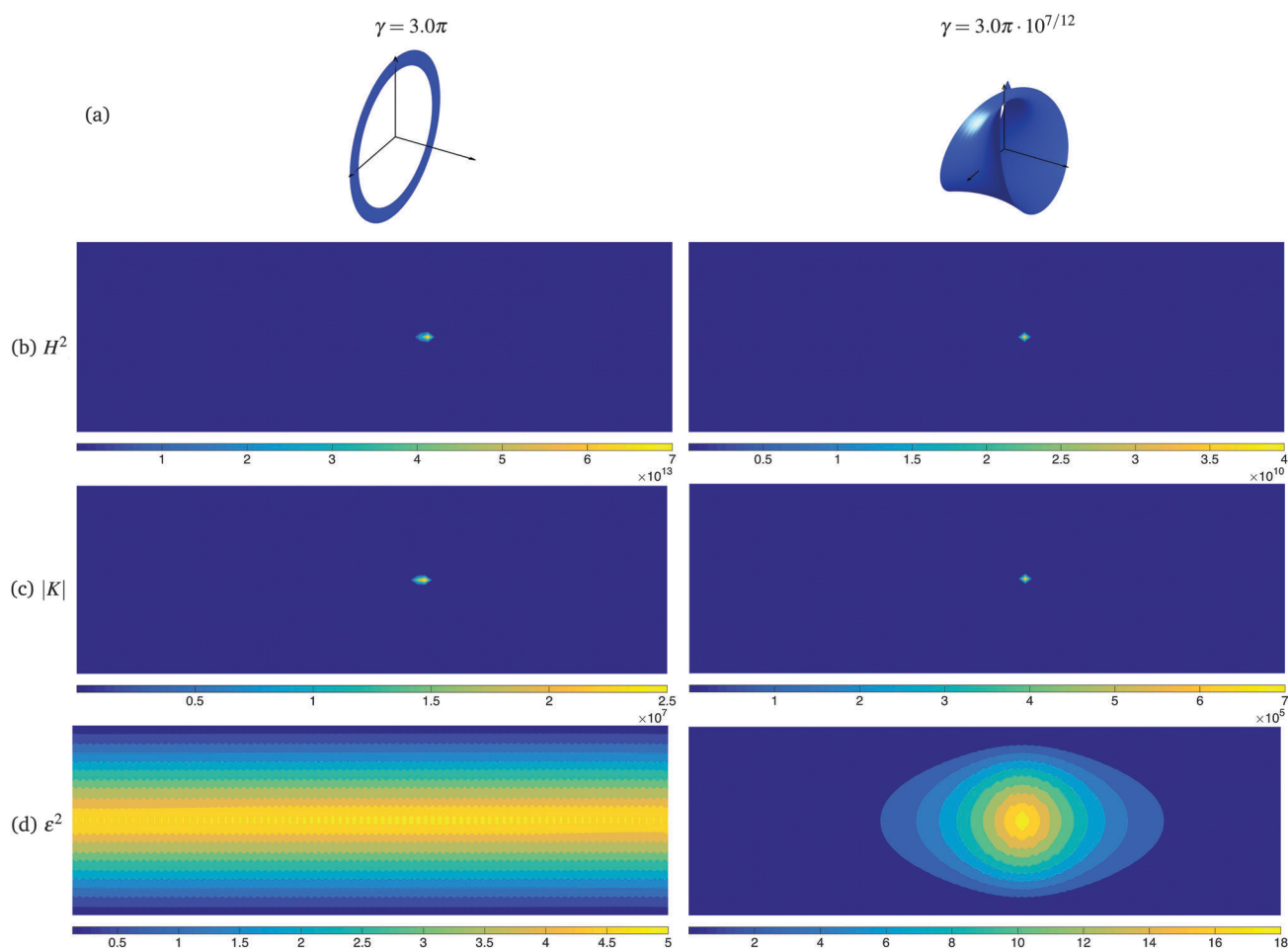
Fig. 8 Both mean and Gaussian curvature are concentrated along the intersection of degenerate self-intersecting achiral bands: (a) collapsed bands colored by stretchability as in Fig. 2, (b) square H^2 of the mean curvature H, (c) magnitude $|K|$ of the Gaussian curvature K, and (d) square ε^2 of the strain ε of collapsed Möbius bands for $a = \pi$ and different values of the FvK number γ. Different scales are adapted individually to capture the entire range of relevant values.

into a two-dimensional flat annulus, the values of H^2, $|K|$, and ε^2 are maximal along the midline of the band, which is the line along which folding occurs.

3.5 Lines of curvature

Differences in the distributions of curvature and stretch are mirrored by the lines of curvature, which are curves with tangent vectors that align with a principal direction at every point. Plots of these curves for representative combinations of the FvK number γ and aspect ratio a are provided in Fig. 9. To construct these plots, we determine the vector field of principal directions and approximate the lines of curvature by computing the relevant streamlines.

The least regular grid occurs for $\gamma = 3.0\pi \times 10^7$. The improvement in regularity that occurs as γ decreases indicates that smaller gradients of the curvature correspond to smaller strain gradients. Consistent with the previous discussion, bands made of stretchable materials therefore exhibit reduced concentrations of bending.

The lines of curvature of a collapsed band form a nearly regular grid but curve sharply near the intersection of the band (which coincides with the previously mentioned axis of symmetry). In the absence of collapse, for bands made of stretchable materials we otherwise observe similar behavior. However, lines of curvature bordering the axis of symmetry of such a band are smoother.
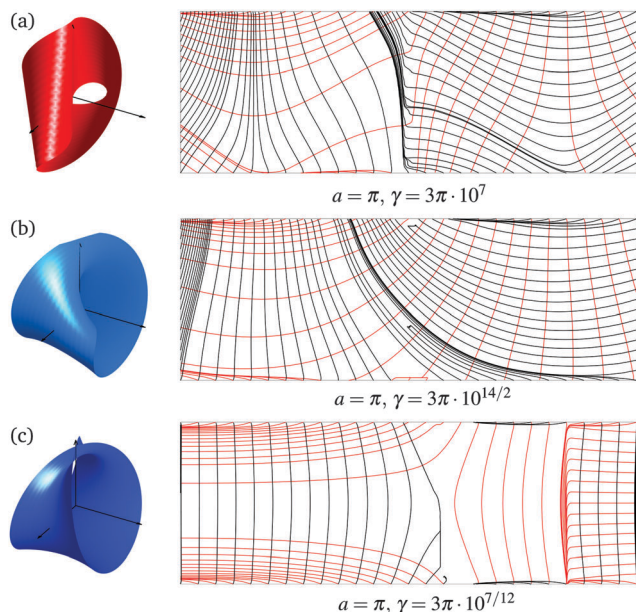
Fig. 9 Lines of curvature are symmetric and trace out a nearly regular grid for bands made of stretchable materials, indicating reduced concentrations of bending-energy density: lines of curvature for three representative combinations of γ and a are shown on a rectangular strip with the corresponding equilibrium shape provided on the left. (a) Developable shapes have pronounced lines of curvature along the length of the band with nearly straight lines of curvature along their widths. (b) For bands made of stretchable materials, shapes with circular midlines also have nearly straight lines of curvature; however any such band curves more gradually near its axis of symmetry. (c) Collapsed shapes have nearly straight lines of curvature with a sharp curve near the center of the intersection.

4 Conclusions and discussion

Using a discrete, lattice-based model, we confirm analytical results for the distributions of curvature and torsion on the midlines of Möbius bands[21] along with results qualitatively similar to those obtained for continuum models.[20,22,23] By analogy to the effect of writhe,[33,34] we find that twisting strain becomes delocalized if stretching is allowed. To predict macroscopic band shapes for a given material, we establish a connection between stretchability and relevant continuum moduli. This affords insight regarding the practical feasibility of synthesizing Möbius bands from materials with continuum parameters that can be measured experimentally or estimated by upscale averaging.

We find that Möbius bands adopt different characteristic shapes depending on stretchability, as described by the FvK number γ, and aspect ratio a. For sufficiently large values of γ, equilibrated Möbius bands have similar shapes and appear to be nearly developable, regardless of the values of a. In such bands, the bending-energy density is highly localized in regions where the curvature gradients are high. For smaller values of γ, the centerlines of equilibrated bands appear to be more circular and planar. The bending-energy density of such bands is therefore delocalized. Shape differences becomes more pronounced when a is reduced. These parameter combinations provide reasonable target shapes and strategies for the guided assembly and synthesis of Möbius bands. In particular, we find that highly stretchable bands have lower energies, indicating that it should be easier to make Möbius bands from more stretchable materials. It is therefore conceivable that Möbius molecules might correspond to these stretchable shapes. For $\gamma > 3\pi \times 10^{7/6}$, we find that the energy becomes increasingly large as a decreases—so that wider bands should be more difficult to make than narrower ones. For $\gamma < 3\pi \times 10^{7/6}$, we find conversely that narrower bands have lower energies; however, for $a = \pi$ and either $\gamma = 3\pi \times 10^0$ or $\gamma = 3\pi \times 10^{7/12}$ they collapse into self-intersecting achiral shapes, which are degenerate Möbius bands. This suggests that highly stretchable bands with small aspect ratios might be unstable and thus impossible to make. For $10^1 \lesssim \gamma \lesssim 10^2$, bands with smaller values of a should, however, be easier to make than those with larger values of a.

Thus, γ and a influence not only the equilibrium shape of a Möbius band but also its ease of guided assembly. Due to the energetically advantageous nature of bands made of stretchable materials, the ability to design and fabricate Möbius bands with nondevelopable shapes might be valuable. These findings could be helpful in a variety of applications and also serve as an archetype for other twisted topologies.

In particular, our results indicate that bands made of stretchable materials are distinguished from bands with developable shapes by lower curvature gradients. Consequently, the extent to which the curvature of a band is homogeneous increases as the FvK number γ decreases. This connection between stretchability, curvature gradients, and shape has implications for the electronic ground state of quantum Möbius bands.[35] In particular, the ground and excited states of a Möbius band determined by

minimizing Wunderlich's functional over a restricted family of midlines were found to exhibit wave functions that are significantly altered by curvature effects.[36] Similarly, curvature has been found to influence electron localization, where deep potential wells arise in connection with singularities of the bending-energy density.[37] Since stretchability and curvature are inextricably linked,[25] our results suggest that the electron localization of a quantum Möbius band is directly related to its stretchability and aspect ratio. For bands made of stretchable materials, the combined influences of nontrivial Gaussian curvature and mean curvature may yield unprecedented effects.

Möbius bands comprised of graphene with architectures that impart stretchability might allow for advances based on Möbius topology. Importantly, the use of graphene Möbius bands for topological insulators has already been investigated.[38]

Also in the quantum realm and taking advantage of Möbius topology, a method to enhance spiral intramolecular charge transfer in Möbius cyclacene for use in novel optical and photoelectric devices has been proposed.[39]

Given the ever-increasing spectrum of applications, the treatment of stretchability and aspect ratio and their implications for the Möbius band presented here may help guide further developments as well as to increase the theoretical understanding of these fascinating objects.

Acknowledgements

References

1 S. Gupta and A. Saxena, A topological twist on materials science, *MRS Bull.*, 2014, **39**, 265–279.
2 M. Fujita, F. Ibukuro, H. Seki, O. Kamo, M. Imanari and K. Ogura, Catenane formation from two molecular rings through very rapid slippage. A Möbius strip mechanism, *J. Am. Chem. Soc.*, 1996, **118**, 899–900.
3 D. Han, S. Pal, Y. Liu and H. Yan, Folding and cutting DNA into reconfigurable topological nanostructures, *Nat. Nanotechnol.*, 2010, **5**, 712–717.
4 S. Tanda, T. Tsuneta, Y. Okajima, K. Inagaki, K. Yamaya and N. Hatakenaka, A Möbius strip of single crystals, *Nature*, 2002, **417**, 397–398.
5 V. A. Osipov, Topological defects in carbon nanocrystals, in *Monastyrsky*, ed. M. I., Topology in Condensed Matter, Springer, Berlin, 2006, pp. 93–116.
6 D. Ajami, O. Oeckler, A. Simon and R. Herges, Synthesis of a Möbius aromatic hydrocarbon, *Nature*, 2002, **417**, 819–821.
7 M. Stepien, L. Latos-Grażyński, N. Sprutta and L. Szterenberg, Expanded porphyrin with a split personality: A Hückel–Möbius aromaticity switch, *Angew. Chem., Int. Ed.*, 2007, **46**, 7869–7873.
8 C. V. Jennings, K. J. Rosengren, N. L. Daly, M. Plan, J. Stevens, M. J. Scanlon, C. Waine, D. G. Norman, M. A. Anderson and

D. J. Craik, Isolation, solution structure, and insecticidal activity of kalata B2, a circular protein with a twist: do Möbius strips exist in nature?, *Biochemistry*, 2005, **44**, 851–860.
9 C. K. L. Wang, R. J. Clark, P. J. Harvey, K. J. Rosengren, M. Cemazar and D. J. Craik, The role of conserved glu residue on cyclotide stability and activity: a structural and functional study of kalata B12, a naturally occurring Glu to Asp mutant, *Biochemistry*, 2011, **50**, 4077–4086.
10 A. B. Smith, N. L. Daly and D. J. Craik, Cyclotides: a patent review, *Expert Opin. Ther. Pat.*, 2011, **21**, 1657–1672.
11 A. G. Poth, L. Y. Chan and D. J. Craik, Cyclotides as grafting frameworks for protein engineering and drug design applications, *Biopolymers*, 2013, **100**, 480–491.
12 M. Sadowsky, Ein elementarer Beweis für die Existenz eines abwickelbaren Möbiusschen Bandes und die Zurückführung des geometrischen Problems auf ein Variationsproblem, *Sitzungsber. Preuss. Akad. Wiss., Phys.-Math. Kl.*, 1930, **22**, 412–415.
13 D. F. Hinz and E. Fried, Translation of Michael Sadowsky's paper "An elementary proof for the existence of a developable Möbius band and the attribution of the geometric problem to a variational problem", *J. Elast.*, 2015, **119**, 3–6.
14 M. Sadowsky, Theorie der elastisch biegsamen undehnbaren Bänder mit Anwendungen auf das Möbius'sche Band, in Oseen, ed. A. C. W. and W. Weibull, *Proceedings of the 3rd International Congress of Applied Mechanics, Stockholm*, AB. Sveriges Litografiska Tryckerier, Stockholm, 1930, vol. 2, 444–451.
15 D. F. Hinz and E. Fried, Translation and interpretation of Michael Sadowsky's paper "Theory of elastically bendable inextensible bands with applications to the Möbius band", *J. Elast.*, 2015, **119**, 7–17.
16 M. Sadowsky, Die Differentialgleichungen des Möbiusschen Bandes, Jahresbericht der Deutschen Mathematiker Vereinigung, (Report on the Annual Conference, Prague, 16–23 Sept., 1929), 1930, **39**, 49–51, 2. Abteilung.
17 D. F. Hinz and E. Fried, Translation of Michael Sadowsky's paper "The differential equations of the Möbius band", *J. Elast.*, 2015, **119**, 19–22.
18 W. Wunderlich, Über ein abwickelbares Möbius band, *Monatsh. Math.*, 1962, **66**, 276–289.
19 R. Todres, Translation of W. Wunderlich's, "On a Developable Möbius Band", *J. Elast.*, 2015, **119**, 23–34.
20 L. Mahadevan and J. B. Keller, The shape of a Möbius band, *Proc. R. Soc. London, Ser. A*, 1993, **440**, 149–162.
21 T. Randrup and P. Røgen, Sides of the Möbius strip, *Arch. Math.*, 1996, **66**, 511–521.
22 E. L. Starostin and G. H. M. van der Heijden, The equilibrium shape of an elastic developable Möbius strip, *Proc. Appl. Math. Mech.*, 2007, 7, 2020115.
23 E. L. Starostin and G. H. M. van der Heijden, The shape of a Möbius strip, *Nat. Mater.*, 2007, **6**, 563–567.
24 D. F. Caulfield, D. Gunderson, Paper testing and strength characteristics. in *1988 Paper Preservation Symposium: Capital Hilton, Washington, DC, October 19–21*, 31–40, 1988, TAPPI Press.
25 K. F. Gauss, Disquisitiones generales *circa* superficies curvas, *Comm. Soc. Reg. Sci. Gott.*, 1827, **6**, 99–146.

26 T. T. Ngyuen, R. F. Bruinsma and W. M. Gelbart, Elasticity theory and shape transitions of viral shells, *Phys. Rev. E: Stat., Nonlinear, Soft Matter Phys.*, 2005, **72**, 051923.

27 S. Plimpton, Fast parallel algorithms for short-range molecular dynamics, *J. Comput. Phys.*, 1995, **117**, 1–19.

28 R. E. Goldstein, H. K. Moffatt, A. I. Pesci and R. L. Ricca, Soap-film Möbius strip changes topology with a twist singularity, *Proc. Natl. Acad. Sci. U. S. A.*, 2010, **107**, 21979–21984.

29 S. Fejer and D. Wales, Helix self-assembly from anisotropic molecules, *Phys. Rev. Lett.*, 2007, **99**, 086106.

30 H. S. Seung and D. R. Nelson, Defects in flexible membranes with crystalline order, *Phys. Rev. A: At., Mol., Opt. Phys.*, 1988, **38**, 1005–1018.

31 G. J. Merchant and J. B. Keller, Flexural rigidity of a liquid surface, *J. Stat. Phys.*, 1991, **63**, 1039–1051.

32 M. P. do Carmo, *Differential Geometry of Curves and Surfaces*, Prentice-Hall, New Jersey, 1976.

33 R. Herges, Topology in chemistry: Designing Möbius molecules, *Chem. Rev.*, 2006, **106**, 4820–4842.

34 G. R. Schaller, F. Topić, K. Rissanen, Y. Okamoto, J. Shen and R. Herges, Design and synthesis of the first triply twisted Möbius annulene, *Nat. Chem.*, 2014, **6**, 608–613.

35 V. M. Fomin, S. Kiravittaya and O. G. Schmidt, Electron localization in inhomogeneous Möbius rings, *Phys. Rev. B: Condens. Matter Mater. Phys.*, 2012, **86**, 195421.

36 J. Gravesen and M. Willatzen, Eigenstates of Möbius nano-structures including curvature effects, *Phys. Rev. A: At., Mol., Opt. Phys.*, 2005, **72**, 032108.

37 A. P. Korte and G. H. M. van der Heijden, Curvature-induced electron localization in developable Möbius-like nano-structures, *J. Phys.: Condens. Matter*, 2009, **21**, 495301.

38 Z. L. Guo, Z. R. Gong, H. Dong and C. P. Sun, Möbius graphene strip as a topological insulator, *Phys. Rev. B: Condens. Matter Mater. Phys.*, 2009, **80**, 195310.

39 R.-L. Zhong, H.-L. Xu, Z.-M. Su, Z.-R. Li, S.-L. Sun and Y.-Q. Qiu, Spiral intramolecular charge transfer and large first hyperpolarizability in Möbius cyclacenes: New insight into the localized π electrons, *ChemPhysChem*, 2012, **13**, 2349–2353.